Beeskow-Strauch, B., Schicks, J. M. (2012): The driving forces of guest substitution in gas hydrates - A laser Raman study on CH4-CO2 exchange in the presence of impurities. - Energies, 5, 2, 420-437

DOI: 10.3390/en5020420

Energies **2012**, *5*, 420-437; doi:10.3390/en5020420

OPEN ACCESS

energies

ISSN 1996-1073

www.mdpi.com/journal/energies

Article

The Driving Forces of Guest Substitution in Gas Hydrates—A Laser Raman Study on CH_4-CO_2 Exchange in the Presence of Impurities

Bettina Beeskow-Strauch * and Judith Maria Schicks

Helmholtz Centre Potsdam, German Research Centre for Geosciences (GFZ), Telegrafenberg, 14473 Potsdam, Germany; E-Mail: schick@gfz-potsdam.de

* Author to whom correspondence should be addressed; E-Mail: betti@gfz-potsdam.de; Tel.: +49-331-288-1425; Fax: +49-331-288-1474.

Received: 15 December 2011; in revised form: 2 February 2012 / Accepted: 14 February 2012 / Published: 22 February 2012

Abstract: The recovery of CH_4 gas from natural hydrate formations by injection of industrially emitted CO_2 is considered to be a promising solution to simultaneously access an unconventional fossil fuel reserve and counteract atmospheric CO_2 increase. CO_2 obtained from industrial processes may contain traces of impurities such as SO_2 or NO_x and natural gas hydrates may contain higher hydrocarbons such as C_2H_6 and C_3H_8. These additions have an influence on the properties of the resulting hydrate phase and the conversion process of CH_4-rich hydrates to CO_2-rich hydrates. Here we show results of a microscopic and laser Raman *in situ* study investigating the effects of SO_2-polluted CO_2 and mixed CH_4-C_2H_6 hydrate on the exchange process. Our study shows that the key driving force of the exchange processes is the establishment of the chemical equilibrium between hydrate phase and the surrounding phases. The exchange rate is also influenced by the guest-to-cavity ratio as well as the thermodynamic stability in terms of *p*-*T* conditions of the original and resulting hydrate phase. The most effective molecule exchange is related to structural changes (sI-sII) which indicates that hydrate decomposition and reformation processes are the occurring processes.

Keywords: gas hydrate; CH_4-CO_2 exchange; SO_2; C_2H_6; chemical equilibrium; sI-sII conversion

1. Introduction

Methane trapped in ocean and permafrost gas hydrate deposits is thought to be a fossil fuel reserve on the order of at least all conventional known reservoirs and may turn into a future energy source [1,2]. Published estimates of the last ten years vary, depending on the presumptions, between 0.2×10^{15} m^3 STP (standard temperature pressure) and 120×10^{15} m^3 STP CH_4 bonded in hydrate-bearing sediments [3,4]. Even the most conservative assumptions show an enormous energy potential when compared to conventional gas reserves of 0.15×10^{15} m^3 STP [5]. The gas production from hydrate-bearing sediments is, however, still a technical challenge. In order to release gas from hydrate-bearing sediments it is necessary to decompose the gas hydrate. In principle, this can be realized by distortion of the mechanical equilibrium (pressure reduction), the thermal equilibrium (heating) or the chemical equilibrium (e.g., injection of inhibitors or CO_2). The latter, coupling of controlled CH_4 gas production and CO_2 sequestration is often seen as an ideal solution to the demand for fossil fuel and has been proposed as an effective means of counteracting atmospheric CO_2 increase. The replacement of CH_4 in hydrate cages by CO_2 might also maintain the stability of a hydrate field to avoid potential slope slides and subsidence.

In theory, the exchange is simply possible because CO_2 is a very good hydrate forming molecule and the resulting CO_2 hydrate is stable at even higher temperatures at given pressure conditions compared to pure CH_4 hydrate. However, in practice some other aspects come into play which have not been considered in the past.

First, pure CH_4 hydrates are very rare in natural environments [6]; in fact, almost all natural gas hydrate deposits discovered so far contain minor proportions of higher hydrocarbons or other traces, such as CO_2 or H_2S. They form, depending on guest molecule concentrations, different crystallographic structures. Structure I (sI) gas hydrates are CH_4-rich, but may also include small fractions of CO_2 and H_2S. These hydrates predominantly originate from microbial CH_4 production and are the most abundant hydrate structure on earth [7]. They have been reported for instance for many deposits in the Hydrate Ridge offshore Oregon or in the Blake Ridge [8,9]. Structure II (sII) and structure H (sH) hydrates form primarily from gas molecules of thermogenic origin and contain compounds from CH_4 up to butane and up to hexane for sII and sH, respectively. They have been found in the northern Gulf of Mexico and the northern Cascadia Margin [10,11].

Second, industrially emitted *pure* CO_2 does not exist. The three methods prior to CO_2 capture are oxyfuel-, pre- and post-combustion, whereby only the latter is considered a well-developed technology [12]. To separate and capture CO_2 from the gas stream a range of methods currently exist based on physical and chemical processes, including absorption, adsorption, membranes and cryogenics [13]. Industrially emitted CO_2 includes typically further contaminants such as SO_2 and NO_2. SO_2 impurities are largely removed by gas scrubbing with alkaline solid or solution sorbents. NO_2 is mostly removed using catalytic reduction with NH_3, producing N_2 and H_2O. For a realistic benefit-cost ratio the cleaning process is barely complete and the resulting CO_2 still contains traces of impurities [14].

Third, the replacement of CH_4 with CO_2 in the hydrate phase under lab conditions has been investigated by several groups. Depending on experimental conditions and setups, the reported

exchange of CH_4 by means of CO_2 replacement in the hydrate phase varies widely: between 15% CH_4 within 800 h and 80% after only 15 h [15,16].

But the CO_2 hydrate durability is only assured as far as the chemical environment does not change which is not the case in the presence of a proximate CH_4 gas source. The compositional dis-equilibrium between hydrate phase and environment caused by the high CH_4 concentration in the surrounding fluid—and with this a difference regarding the chemical potential in both phases—might induce a decomposition of the CO_2 hydrate.

The follow-up scenario—the possible CO_2 hydrate dissolution and renewed CH_4 hydrate formation from the original source—has been investigated recently by Schicks *et al.* [17], demonstrating that conversion of CH_4 hydrate into CO_2 hydrate is reversible, when the CO_2 hydrate is exposed to a hydrocarbon atmosphere.

2. Results and Discussion

To converge on a real production scenario by means of CO_2 sequestration into CH_4 hydrate reservoirs, not only pure CH_4 and CO_2 have been used for this study. Mixed hydrates, formed from a CH_4-C_2H_6 mixture (7% C_2H_6) and impure CO_2 (containing 1% SO_2) have been tested for the exchange process in both directions.

C_2H_6 is a common component of natural gas hydrates and causes, in concentrations used here, the formation of a sII hydrate [18]. This study aims to examine whether structural changes occur during exchange reactions or the hydrate lattice structure stays unaffected by guest molecule exchange. Furthermore, the influence of potential structural changes on exchange efficiency can be determined.

The CO_2-impurities of 1% SO_2 shall be deemed to be industrially emitted CO_2. Previous experiments have shown that SO_2 is a good hydrate former and that mixed CO_2-SO_2 hydrates exceed the thermodynamic stability of a pure CO_2 hydrate in terms of *p-T* stability [19,20]. Therefore, the influence of SO_2 on the exchange reactions has been studied too.

By using this variety of gas- and gas hydrate compositions, our work furthermore provides an insight into driving forces for guest molecule exchange.

2.1. Experiments

As shown in Figure 1, the overall experimental procedure consists of three parts, where the first part comprises the hydrate formation. This part of the experiment, which is described in the Experimental section, usually takes two days. As it has no relevance for this study of exchange behavior in gas hydrates it is not considered in the following descriptions and diagrams. In all experiments the duration of the primary exchange has been scheduled for four days, the return exchange extends to about twice the time span. This experimental time scale has been chosen in order to approximate on real conditions where natural gas production from a gas hydrate deposit is a short event compared to the subsequent storage of the newly formed CO_2-rich hydrate in an environment which is potentially enriched in CH_4 dominated natural gas.

For this study we use the term “exchange” to describe the substitution/replacement of guest molecules in the hydrate phase with gas molecules of the adjacent gas phase and *vice versa*. It does not necessarily mean the replacement of gas molecules in one and the same hydrate cavity or, in other

words, we assume that hydrate cavities have to be destroyed at least in parts to release gas molecules and to encase new guests. We also use the term "conversion" which here implies the general alteration of the hydrates with respect to their composition and structure. It comprises both the change from single hydrates to mixed hydrate as well as the change of the hydrate structure from sI to sII and *vice versa*. In similar context the terms "exchange or conversion reaction/process" are used. We also differentiate between hydrate-forming gas and exchange gas whereby hydrate forming gas is used during hydrate preparation and during return-conversion and exchange gas during the first conversion reaction. The term "reaction" should not suggest a chemical process but a response to a stimulus.

Figure 1. Schematic illustration of the experimental process, subdivided into preparation, conversion and return-conversion. Temperatures *versus* time as well as gas composition (in %) are exemplarily shown for the CH_4-CO_2 exchange.

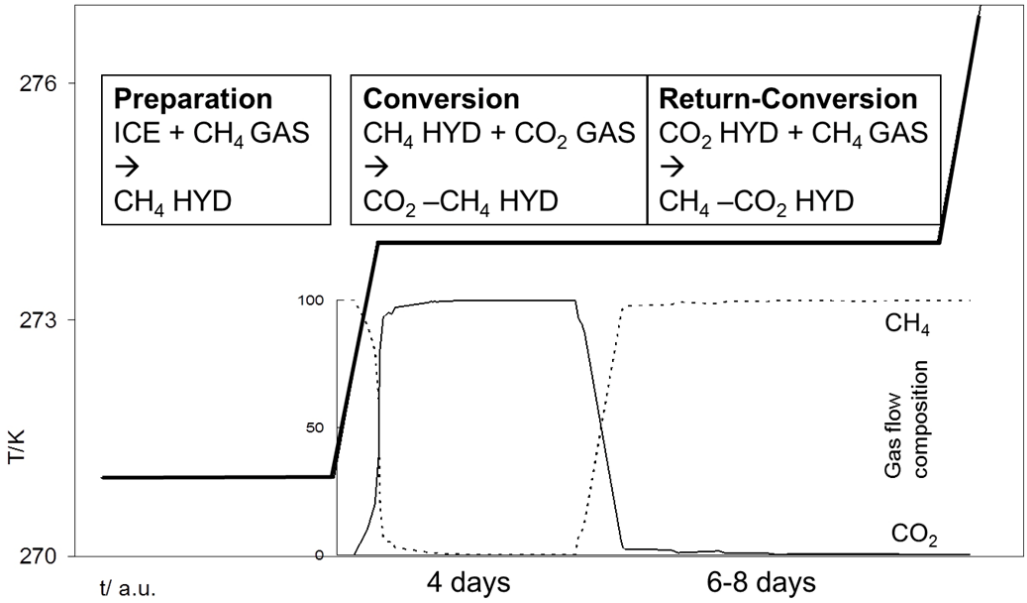

2.1.1. The CH_4-CO_2 Exchange

In the reference experiment pure substances have been used (Figure 2a). The experiment started with the preparation of a pure sI CH_4 hydrate. The exchange process has been induced by offering pure CO_2 gas. For that, the gas flow has been changed from CH_4 to CO_2. After about four days of exposing the hydrate phase to CO_2 gas, the reaction ceased and results in a mixed CH_4-CO_2 hydrate with relative CO_2 concentrations between 40% and 70% in the hydrate phase.

On the reverse exchange, offering CH_4 again to the newly formed mixed CH_4-CO_2 hydrate, no complete removal of the CO_2 has been observed within eight days. In fact, the conversion reactivity slowed down after about five days and exhibited a stationary state with between 10% and 30% CO_2 in the mixed CH_4-CO_2 hydrate within the following days.

2.1.2. The CH_4–CO_2-SO_2 Exchange

On the second sequence of experiments, simple CH_4 hydrate has been exposed to a CO_2-SO_2 gas mixture (Figure 2b). After four days, the hydrate composition reached values of up to 15% SO_2 and between 45% and 70% CO_2. The supplier gas stream was then changed back to pure CH_4 and the relative concentrations of the CH_4-CO_2-SO_2 hydrate determined for about six days. Already after one day, the relative concentrations leveled out to values of 12% to 40% CO_2 and 2% to 12% SO_2. The respective CH_4 concentrations varied between 50 and 85%. Because SO_2 is a good hydrate former it became strongly enriched in the hydrate phase. While only one percent was offered by the gas phase, up to 15% have been detected in the hydrate phase. This was a result of the continuous gas flow during the experimental procedure which allowed a permanent supply with feed gas and accordingly enrichment in the hydrate phase.

Figure 2. (**a**) Changes in hydrate composition (red—CH_4, green—CO_2) with time when CH_4 hydrate is exposed to CO_2 and *vice versa*. The red and green areas emphasize the heterogeneity of the hydrate phase. At the starting point (time zero) the prepared CH_4 hydrate was exposed to exchange gas, the dashed line marks the time when the gas composition has been changed back to the initial hydrate forming gas. (**b**) Changes in hydrate composition (red—CH_4, green—CO_2, small green diamonds—SO_2) with time when CH_4 hydrate is exposed to CO_2-SO_2 gas and *vice versa*. (**c**) Changes in hydrate composition (red—CH_4, small red circles—C_2H_6, green—CO_2) with time when CH_4-C_2H_6 hydrate is exposed to CO_2 gas and *vice versa*. (**d**) Changes in hydrate composition (red—CH_4, small red circles—C_2H_6, small green diamonds—CO_2, plus—SO_2) with time when CH_4-C_2H_6 hydrate is exposed to CO_2-SO_2 gas and *vice versa*.

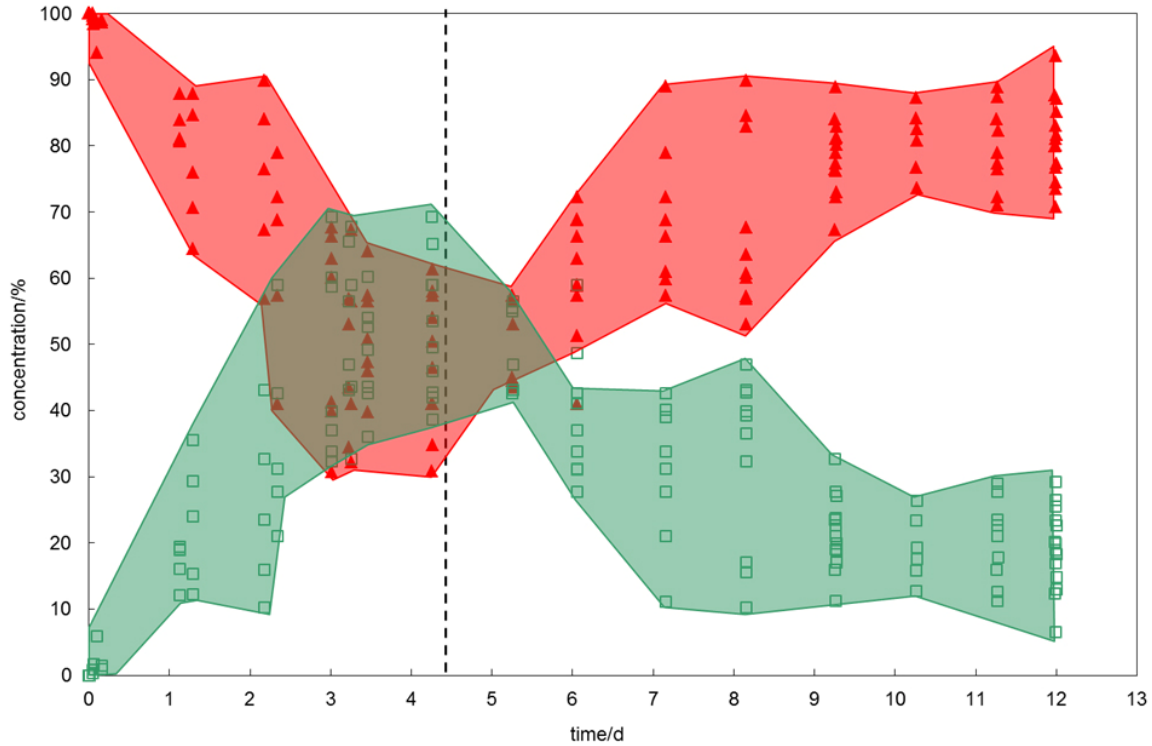

(**a**)

Figure 2. *Cont.*

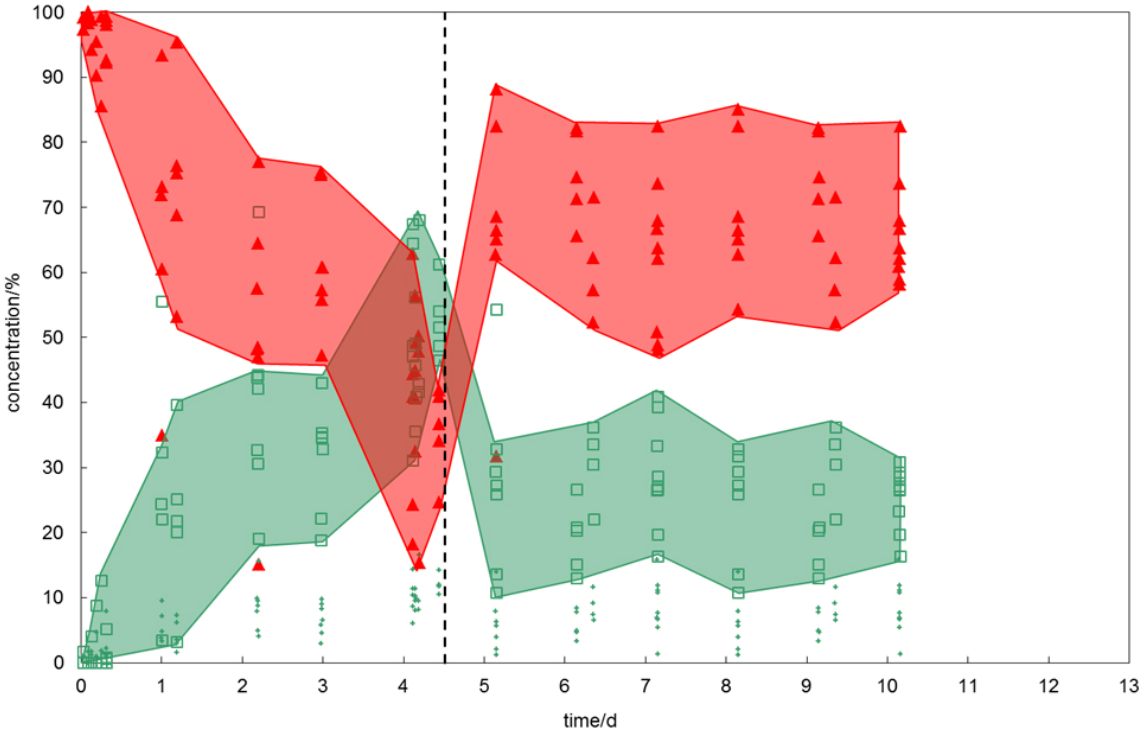

(**b**)

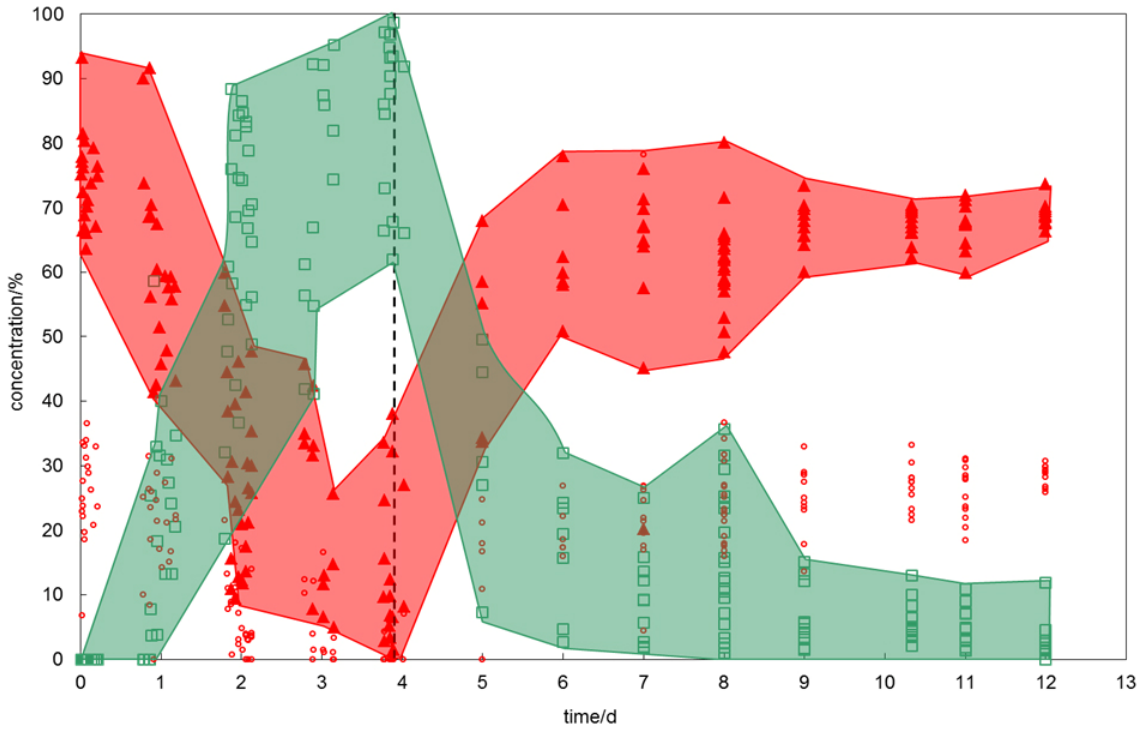

(**c**)

Figure 2. *Cont.*

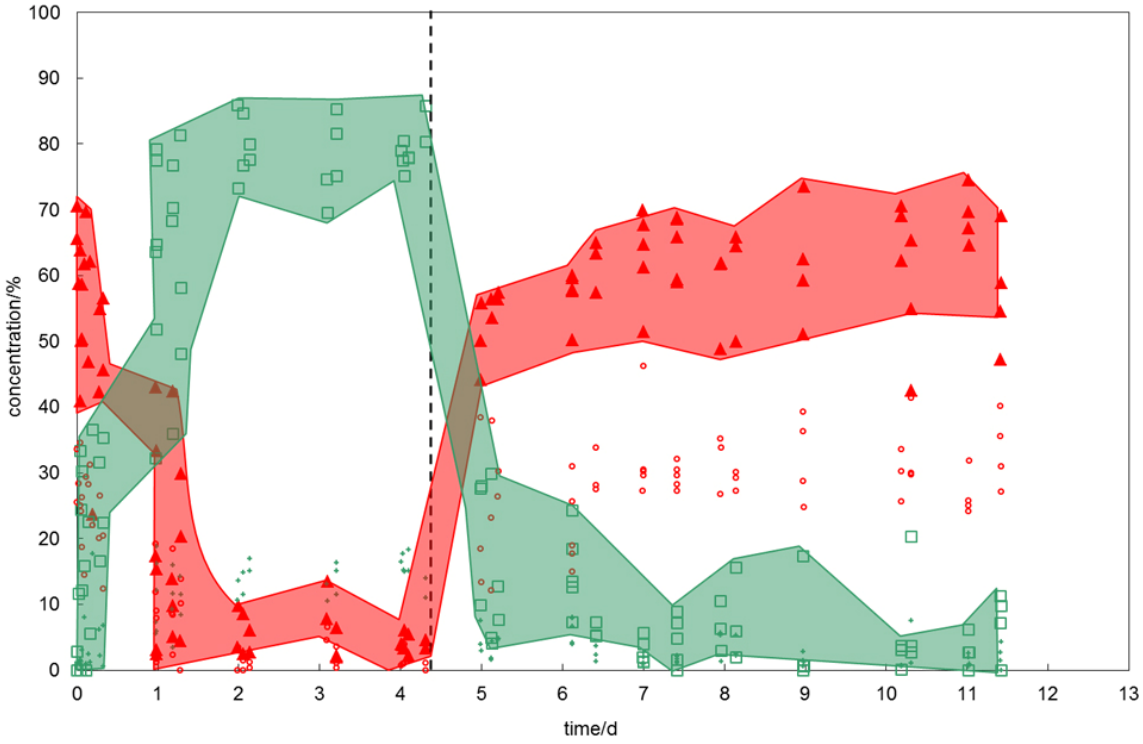

(d)

2.1.3. The CH_4-C_2H_6–CO_2 Exchange

For this experiment, pure CO_2 gas has been provided to a mixed CH_4-C_2H_6 hydrate (Figure 2c). The starting composition of the CH_4-C_2H_6 hydrate showed a strong enrichment of C_2H_6 in the hydrate lattice. Although the feed gas has offered only 7% C_2H_6, up to 35% have been incorporated into the hydrate lattice. The initial CH_4-C_2H_6 hydrates were sII hydrates, evident from the peak positions of the Raman bands (see explanation and Raman spectra below).

On offering pure CO_2, the magnitude of the exchange reaction exceeded that of previously discussed experiments using simple CH_4 hydrate. The newly formed mixed CH_4-CO_2 hydrates showed a CO_2 content of more than 60%. Pure CO_2 hydrates were also detected. The concentration of C_2H_6 decreased to values below detection limit. In the course of the conversion, the initial sII hydrate has been transformed into sI hydrate marked by the change in Raman peak position.

During the reverse exchange, the CO_2 concentration in the hydrate decreased rapidly and the hydrate composition reached, already after one day, a level of 60% to 80% CH_4, 20% to 30% C_2H_6 and only 0 to 15% residual CO_2. These values remained constant until the end of the experiment. Furthermore, the Raman spectra indicated a reformation to sII hydrate.

2.1.4. The CH_4-C_2H_6–CO_2-SO_2 Exchange

Here impure variations of gas and hydrate have been combined (Figure 2d). The results are similar to that of the previous experiment but the effects are even more pronounced. The initial mixed CH_4-C_2H_6 hydrate contained 20% to 35% C_2H_6 and exhibited sII characteristics on the Raman band positions.

On offering CO_2-SO_2 gas, the molecule exchange occurred rapidly and the final (after four days) hydrate composition showed CH_4 and C_2H_6 concentrations of less than 10%, up to 90% CO_2 and up to 20% SO_2 in the hydrate structure. The hydrate has converted into sI.

When offering the CH_4-C_2H_6 gas to the newly formed hydrate, the structure changed again into a sII hydrate. The conversion rate was high for the first day but for the remaining six days the system reached a stationary state with a relatively constant hydrate composition comprising 50% to 75% CH_4, 25% to 40% C_2H_6, 0% to 15% CO_2 and up to 5% SO_2.

In Figure 2a–d it is noticeable that the compositional data of the exchange reaction are inhomogeneous. If the replacement reaction is considered a surface process, this scattering mirrors different stages of the replacement process, whereby unreacted or less reacted material occurs in the subsurface region [21]. Despite much effort to apply the similar procedure when focusing on a hydrate crystal, we cannot exclude variations caused by different focus depth, especially given the fact that the hydrate crystal morphology varies highly.

2.2. The Raman Spectra

Exemplarily, typical spectra of the investigated guest molecules at different experimental stages of the CH_4-C_2H_6–CO_2-SO_2 exchange are summarized in Table 1 and shown in Figure 3.

Table 1. Summary of Raman shifts for molecules measured in this study.

Molecule	**Vibrational Mode**		**Raman Peak Positions (cm^{-1})**				
			gas	sI hydrate		sII hydrate	
				5^{12}	$5^{12}6^2$	5^{12}	$5^{12}6^4$
Methane	υ_1	C-H sym. stretch	2917	2915	2904	2915	2904
Ethane	υ_3	C-C stretch	994		1001		993
	υ_1	CH_3 sym. stretch	2900		2890		2887
	$2\upsilon_{11}$	CH_3 d-stretch	2955		2946		2942
Carbon dioxide	υ_1	sym. stretch (O–C–O)	1285		1275		1275
	$2\upsilon_2$	bending overtone	1388		1381		1381
Sulphur dioxide	υ_1	S-O sym. stretch	1151	1157	1147		1147

For completeness, the typical Raman spectra of the investigated molecules in the gaseous state are shown Figure 3a–c. The Raman signal of C_2H_6 can be determined at 994 cm^{-1}, 2900 cm^{-1} and 2955 cm^{-1} and the CH_4 peak position has been detected at 2917 cm^{-1}. For CO_2 the two Fermi diads occur at 1285 cm^{-1} and 1388 cm^{-1}, the SO_2 Raman band appears at 1151 cm^{-1}. At the beginning of the exchange experiment (Figure 3d–f; 4 min after offering the exchange gas CO_2-SO_2), the mixed CH_4-C_2H_6 hydrate is predominant and occurs in form of sII hydrate. The structure determination is based on the C_2H_6 vibrational modes at 993 cm^{-1}, 2887 cm^{-1} and 2942 cm^{-1} which can be assigned to C_2H_6 encased in the large cavities of sII as well as the position of the CH_4 bands at 2904 cm^{-1} and 2915 cm^{-1} which can be assigned to CH_4 in the large and small cavities, with a strong dominance of the latter. These observations are in good agreement with Hester *et al.* [22]. At this stage, the Raman bands of SO_2 at 1151 cm^{-1} and CO_2 at 1285 cm^{-1} and 1388 cm^{-1} are small and indicative of gas phase appearance only.

Figure 3. Typical Raman bands of the exchange reaction of CH_4-C_2H_6 against CO_2-SO_2. Figure 3a–c shows the typical spectra of investigated molecules in the gas phase. Figure 3d–f shows the Raman spectra during the starting situation with sII mixed CH_4-C_2H_6 hydrate and CO_2-SO_2 gas just arrived. Figure 3g–i shows the spectra of the converted sI mixed hydrate after about two days. Figure 3j–l shows the Raman spectra of the return-conversed hydrate at the end of the exchange experiment.

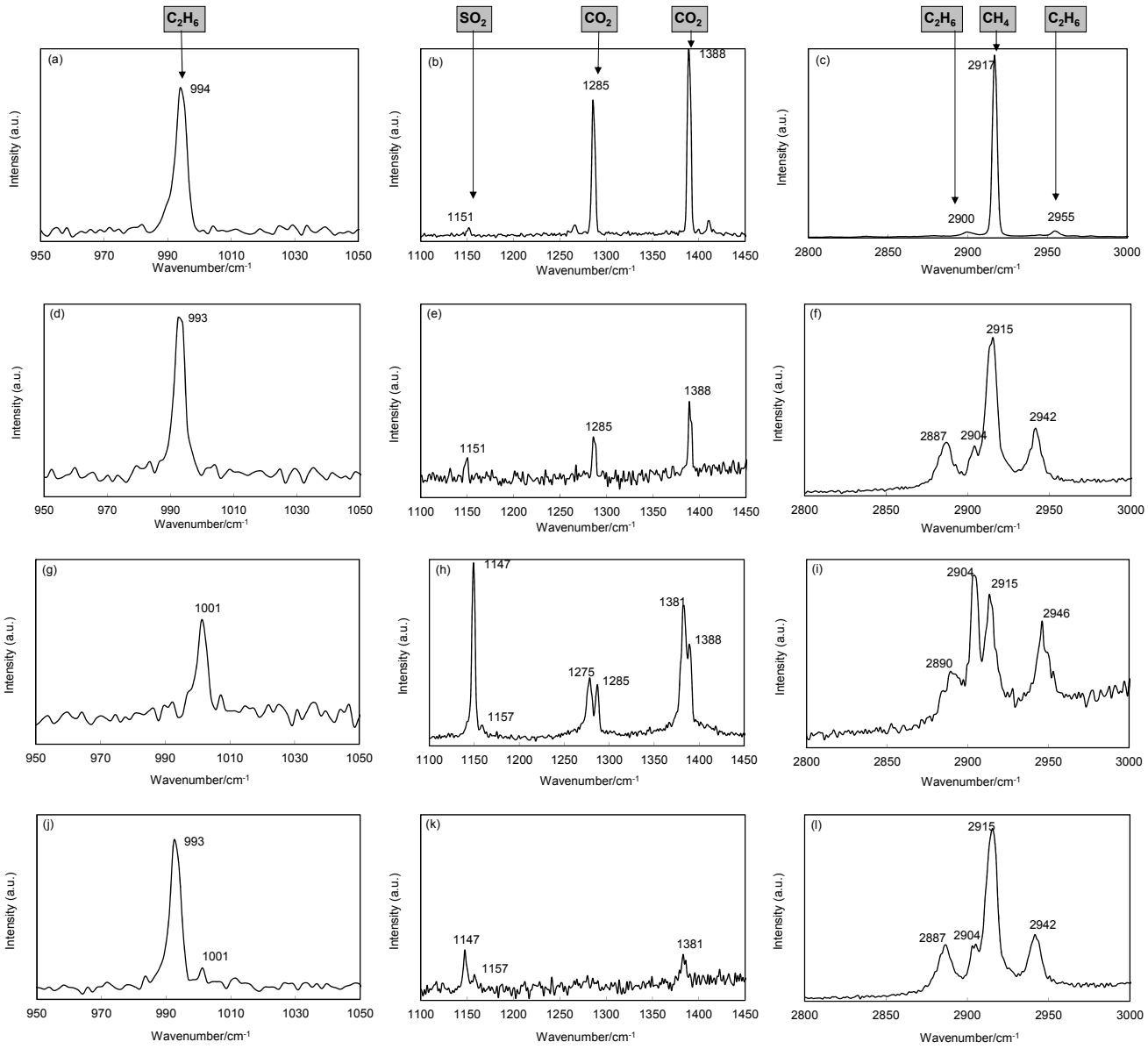

Three days later (Figure 3g–i) the conversion to sI hydrate is evident by the shift in peak positions of C_2H_6 to 1001 cm^{-1}, 2890 cm^{-1} and 2946 cm^{-1}. The observation is in agreement with the appearance of the CH_4 Raman bands, where the band at 2904 cm^{-1}, indicative for large cage occupation, exceeds that of small cages at 2915 cm^{-1}. This is in agreement with findings of Schicks *et al.* [23] and characterizes the typical dominance of large cages in sI structure. The Raman band of gaseous SO_2 has split into two bands at wavenumbers of 1147 cm^{-1} and 1157 cm^{-1} similar to observations of Beeskow-Strauch *et al.* [19], the CO_2 Raman bands appear with two bands at 1275 cm^{-1} and 1381 cm^{-1} which both indicate the incorporation of CO_2 into the hydrate lattice. Additionally, two smaller peaks

with band positions similar to gaseous CO_2 are present. Due to the fact that Raman analysis is not able to distinguish between CO_2 molecules encased in different types of clathrate cavities [24], these bands were assigned as gaseous artifacts. Following the change of gas composition back to the initial hydrate forming gas mixture of CH_4-C_2H_6, a renewed conversion of the hydrate structure from sI to sII is observable by the return of band positions typically for sII hydrates (Figure 3j–l). Contrary to the initially recorded sII Raman signature, relicts of the former sI hydrate structure remain, shown by Raman bands of ethane indicative for sI.

It is not possible to quantify the degree of structural conversion and return-conversion. Based on Raman band intensities and the disappearance of sII Raman bands of ethane, we conclude a complete conversion from sII into sI. This is in good agreement with studies based on PXRD measurements on the conversion of CH_4-C_2H_6 hydrates to CO_2-rich mixed hydrate, which also indicate a complete conversion of sII into sI [17]. The Raman spectra show as well, that the reverse conversion from sI to sII, remains incomplete, which suggests the coexistence of sI, and sII hydrate in the final hydrate.

For all Raman measurements the O-H stretching has been detected in the range from 3000 cm^{-1} to 3800 cm^{-1}. Overall, the O-H Raman feature did not change in peak shape or size to suggest the presence of a liquid water phase. However, the structural changes in the course of guest molecule exchange and hence hydrate conversion from sI to sII and *vice versa* induced a dissociation and reformation of hydrates which likely caused a temporary and spatially limited appearance of free water molecules.

2.3. Discussion of Results

Toward a scenario of CH_4 production and CO_2 storage in gas hydrates we visualized the effectiveness and rate of molecule exchange depending on impurities by plotting the mean values of the relative concentration of CH_4 and CO_2 *versus* time (Figure 4). The data show that impurities in gas or hydrate do increase CH_4 recovery rates and effectiveness but also decrease the ability to retain CO_2 in the hydrate lattice when it comes to a renewed exchange. In particular the addition of C_2H_6 causes an increase in exchange effectiveness. While after four days of pure CH_4-CO_2 exchange about 50% CH_4 remain in the hydrate lattice, less than 10% of CH_4-remnants have been detected in the presence of C_2H_6 impurities. The CO_2 retention is highest for the pure CH_4-CO_2 exchange and decreases with impurity content whereby C_2H_6 impurities result in the strongest CO_2 release. SO_2 impurities in CO_2 cause an increase in molecule exchange rates during the initial phase of the exchange reaction, but result in no significant difference to the final hydrate compositions.

The results of our study indicate three influencing factors for the effectiveness and intensity of the exchange reaction.

Figure 4. Mean values of the relative concentration of CH_4 (left part of the diagram) and CO_2 (right part) in the hydrate phase *versus* time. These visualize the effectiveness and rate of molecule exchange with respect to methane release and CO_2 retention, respectively. (open triangles: exchange of CH_4–CO_2; full triangle: exchange of CH_4–CO_2-SO_2; open circles: CH_4-C_2H_6–CO_2; full squares: exchange of CH_4-C_2H_6–CO_2-SO_2). The dashed line indicates the change of gas flow from initially CO_2-rich to finally CH_4-rich.

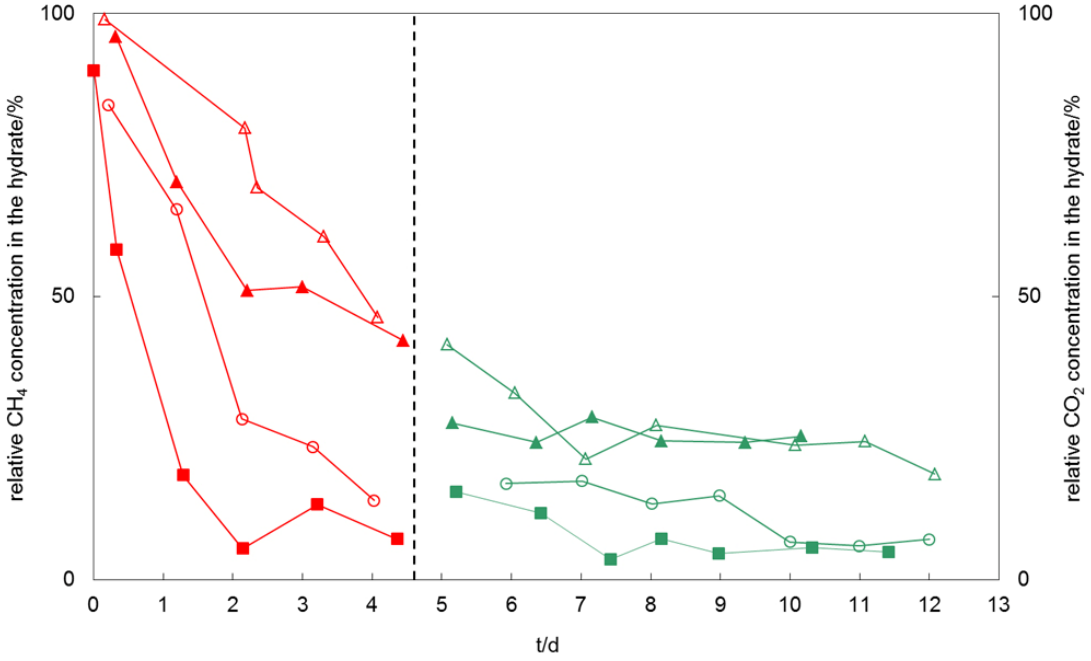

2.3.1. Thermodynamic *p-T* Stability

By comparison of the *p-T* conditions of the phase boundaries, CO_2 hydrate is stable at higher temperatures at given pressure compared to simple CH_4 hydrate [25]. Accordingly, the phase boundaries of mixed CO_2-CH_4 hydrates fall in between the two phase boundary lines for simple CO_2 and CH_4 hydrates (Figure 5).

Impurities of 1% SO_2 in the gas phase increase the *p-T* stability field of the resulting CO_2-rich mixed hydrate, compared to simple CO_2 hydrate. This may lead to the assumption that, if the aim for thermodynamic stability in terms of *p-T* conditions is the key driving force for the exchange reaction, the exchange effectiveness will be intensified in presence of SO_2. In fact, we observed a comparatively rapid conversion rate at the beginning of the exchange experiment but the overall exchange effectiveness remains unaffected. This suggests that a larger *p-T* stability area might be relevant for the initiation of the exchange reaction.

The mixed CH_4-C_2H_6 hydrate is also stable at higher temperatures at a given pressure compared to simple CH_4 hydrate. The stability conditions for the chosen CH_4-C_2H_6 hydrate with respect to temperature and pressure are close to that of pure CO_2 hydrate. This finding may imply a lower exchange rate. However, the exchange rate of mixed CH_4-C_2H_6 hydrates to CO_2-rich hydrate exceeds that of pure CH_4 hydrates. This indicates that the driving force is the aim for chemical equilibrium between all phases. The conversion of CH_4-C_2H_6-hydrate to CO_2-rich hydrate and *vice versa* is coupled to structural conversion (sI-sII).

Figure 5. Stability fields of simple CO_2 hydrates (bold green line), mixed CO_2-SO_2 hydrate (fine green line) formed from CO_2(99%)-SO_2(1%) gas mixture, CH_4 hydrate (bold red line) and CH_4(93%)-C_2H_6(7%) hydrates (fine red line). Also shown are the CO_2 vapor-liquid boundary (blue line) and experimental p-T conditions (dots). Data according CSMHyd [25], data of CO_2-SO_2 hydrate stability taken from Beeskow-Strauch [19].

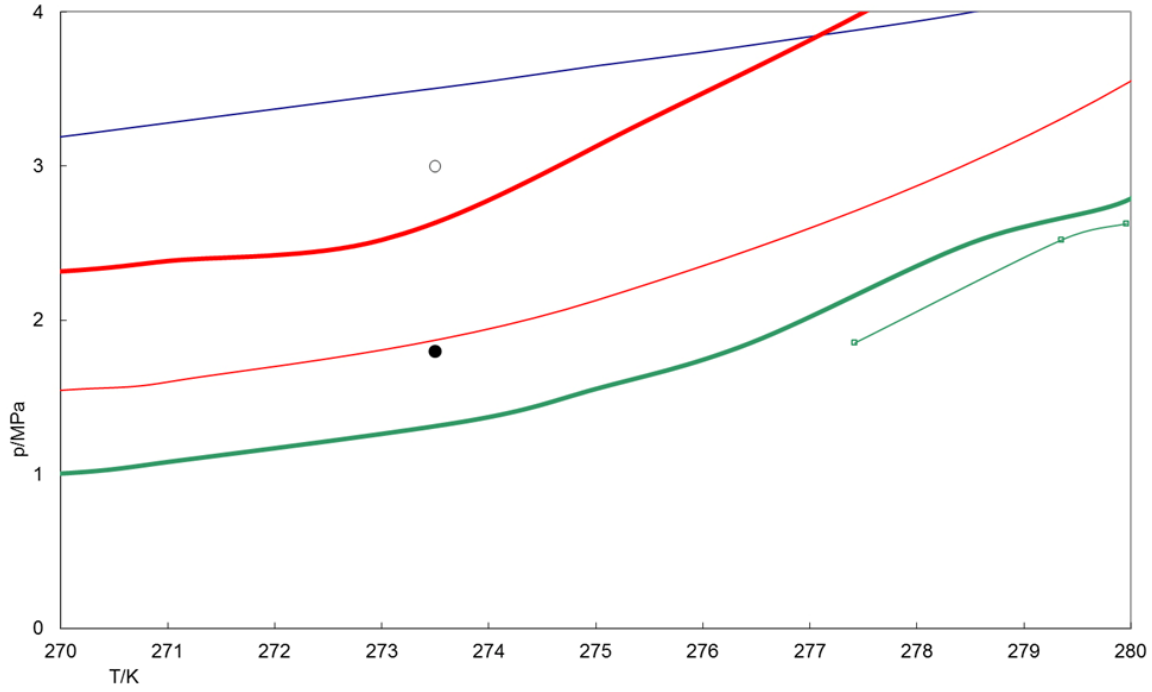

2.3.2. Guest-to-Cavity-Ratio

A unit cell of sI comprises two small cavities (5^{12}) and six large cavities ($5^{12}6^2$), whereas a unit cell of sII consists of sixteen small cavities (5^{12}) and eight large cavities ($5^{12}6^4$). Although both CH_4 and C_2H_6 are individually sI hydrate formers, the binary system of CH_4-C_2H_6 with a ratio of 93/7 is typically observed to form sII hydrates. In fact, CH_4-C_2H_6 mixtures containing 75% to 99% CH_4 form sII hydrates. SII is the preferred structure due to the relative stability of the molecules in the hydrate cages (guest-to-cavity-ratio) together with their ratio of large to small cavities in a unit cell of sII hydrates [18,26]. Hendriks *et al.* [27] explain it invoking the abundance of small cavities in sII hydrates which are stabilized exclusively by CH_4. Therefore, the competition between CH_4 and C_2H_6 for the occupation of large cavities in the hydrate is reduced compared to sI hydrates.

When CO_2 or a mixture of CO_2 and SO_2 gas are offered to the CH_4-C_2H_6 mixed sII hydrate, a conversion to sI hydrate occurs. The reason is the large size of both these newly offered molecules which makes them preferentially suitable for large cages. Consequently, the aim to maximize the number of large cages enforces a structural conversion of sII to sI during the exchange reaction. During the return-exchange the number of CH_4 molecules increases which induces a reverse structural conversion of sI to sII. This conversion, however, remains incomplete resulting in the coexistence of sI and sII structures in the final hydrate. We assume that the ability of CH_4 to occupy large cages of sI attenuates the demand to increase the ratio of small to large cages. It shows that an optimal guest-to-cavity-ratio not necessarily equates with complete structural conversion.

Generally, offering new guest molecules to existing hydrates might cause the impulse for a structural rearrangement to optimize guest-to-cavity-ratios. This restructuring process is attended by a strong molecular disorder which results in a large interface between gas and hydrate phase. In the course of an exchange reaction, it supports an intense molecule exchange between hydrate phase and adjacent gas phase.

2.3.3. Chemical Equilibrium

Guest molecule exchange as well as structural conversion between sI and sII occurs in both directions. This basic finding indicates that the compositional disequilibrium, induced by changes of the surrounding gas phase composition, is the key driving force for the exchange process in gas hydrates. The dominant influence of obtaining an equilibrium of the chemical potential in all phases is especially evident when investigating the return-exchange of the simple CO_2-CH_4 exchange experiment. This reaction can neither be driven due to a "higher stability" of the resulting hydrate phase in terms of *p-T* conditions, nor does CH_4 offer a better guest-to-cavity ratio in large cages. Nevertheless the exchange reaction occurs, with the driving force being the chemical disequilibrium between hydrate and surrounding environment.

3. Experimental Section

The experiments were performed using ready-made certified class 1 gases (gas certification ISO 9001) of pure CO_2, CO_2 + 1% SO_2, pure CH_4 and CH_4 + 7% C_2H_6 supplied by Linde AG. The experiments have been performed by varying gas compositions as shown in Table 2 together with *p-T* conditions of the respective experiments.

Table 2. List of performed experiments that shows the combination of used gas mixtures and respective *p-T* conditions.

Experiment	Combination of Gas Mixtures			Experimental Conditions	
	Preparation: hydrate-forming gas	Conversion: offered exchange gas	Return-conversion: offered exchange gas	p/MPa	T/K
(a)	100% CH_4	100% CO_2	100% CH_4	3	273.5
(b)	100% CH_4	99% CO_2 + 1% SO_2	100% CH_4	3	273.5
(c)	93% CH_4+7% C_2H_6	100% CO_2	93% CH_4 + 7% C_2H_6	1.8	273.5
(d)	93% CH_4+7% C_2H_6	99% CO_2 + 1% SO_2	93% CH_4 + 7% C_2H_6	1.8	273.5

3.1. Experimental Setup

Hydrate clathrate formation and exchange experiments were performed in a small-scale (0.4 cm^3 volume) Hastelloy pressure cell covered with a quartz window. The cell was mounted to an Olympus microscope and attached to a Raman spectroscope (LabRam, Jobin Yvon, 532 DPSS laser, 100 mW). This setup allows both the visual observation of the hydrate behavior together with semi-quantitative analysis (relative concentration of compounds in gas phase and hydrate phase) based on Raman spectra. The non-destructive technique of confocal laser Raman spectroscopy is particularly suited to

analyze individual selected phases. Several Raman spectra at different areas of the sample were taken at certain time slots during the experiment.

The pressure cell is designed to operate in continuous gas flow mode via gas in- and outlet ports. The inflow conduit passes through the cell on a long way to cool down the gas to working temperature prior to entering the sample cell. Temperature control is realized by a thermostat and the temperature is determined with a precision of ±0.1 K. A pressure controller regulates the sample pressure with a precision of ±2% rel. The system pressure was measured with a P3MB pressure transducer (Hottinger Baldwin Messtechnik) with a precision of ±0.01% rel. Prior to the experiment start, air was completely flushed out of the cell system by passing the experimental gas through the entire gas flow system.

Laser Raman spectra of mixed systems can be used to determine the relative molar proportions of the components as described in Beeskow-Strauch *et al.* [19] based on the procedures and the cross section factors published by Burke and Schrötter [28,29]. The integrated band intensities of the specimen are proportional to the number of molecules present in the irradiated volume of the sample. Therefore, comparison of the relative corrected integrated band intensities of the species permits their relative proportions to be determined [30].

3.2. Experimental Process

The experimental process has been subdivided into three parts: (1) the production of the initial hydrate sample, (2) the hydrate conversion using exchange gas injection and (3) the reverse-conversion using the preliminary hydrate-forming gas (see Figure 1, Table 2).

The initial hydrate sample has been produced using fine grained ice, prepared in a cryo-mill and transferred into the pre-cooled pressure cell (<273 K). SEM investigation of the ice indicates a particle size between 10 μm and 30 μm (Figure 6). The pressure cell was sealed and exposed to the chosen gas in a continuous gas stream of 1 mL/min. All experiments were run with a pressure of 3 MPa and 1.8 MPa when using pure CH_4 gas and CH_4-C_2H_6 gas, respectively. Subsequent slow heating to about 274.5 K assured the melting of all ice and the ultimately remaining of only hydrate crystals. At this stage, slight cooling (to 273.5 K) of the system enables hydrate growth close to equilibrium conditions. Raman spectra of the growing clathrates were recorded on a regular basis to observe possible changes in clathrate structure or composition. This part of the experiment lasted several hours until no further changes in hydrate composition were recorded and the system reached a stationary state. The *p*-*T* conditions of the experiments were chosen to retain the gaseous state of aggregation of the test gas and to be within the stability fields of the hydrate phases (see Figure 5).

Figure 6. SEM picture of the prepared fine grained ice. The surface of the ice particle is covered with frost and includes fissures and cracks indicating a large surface area.

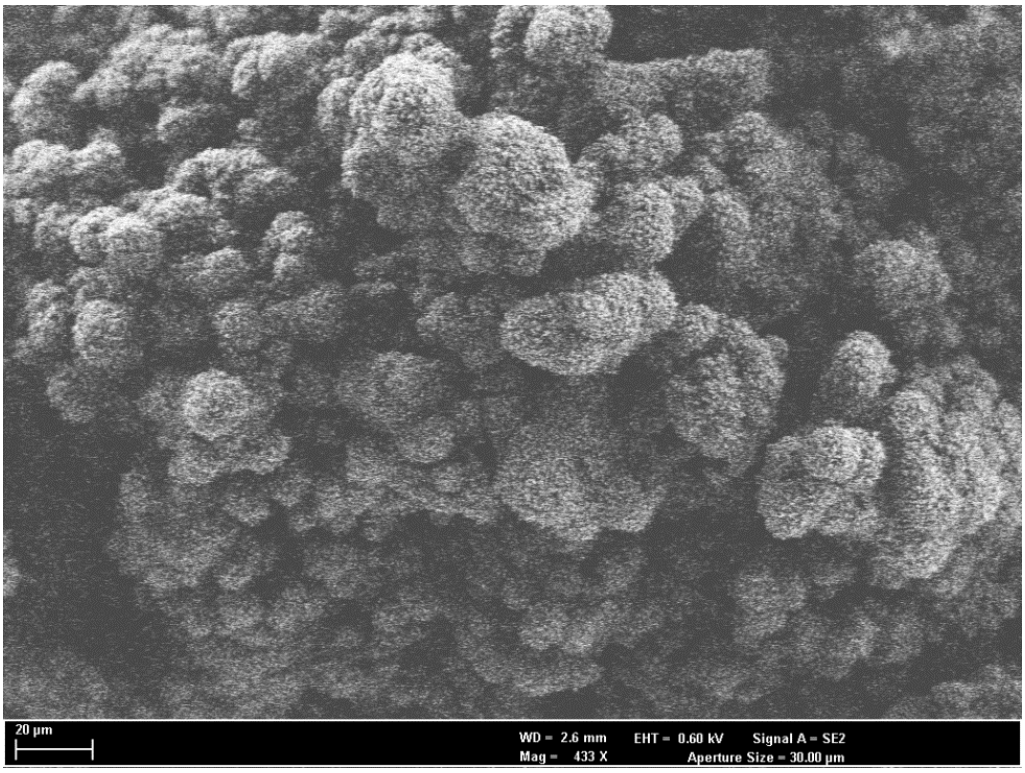

(2) The hydrate conversion process has been initiated by changing the gas composition from the hydrate-forming gas to the exchange gas (in the simplest case: changing from CH_4 to CO_2 gas). For that, the gas inflow route has been isolated from the pressure cell and completely flushed with the exchange gas. The pressure and temperature in the hydrate-containing pressure cell was kept constant. The re-opening of the inflow conduit instantaneously supplies the hydrate sample with the exchange gas and therefore coincides with the start of hydrate conversion. This technique prevents the mixing of hydrate-forming gas and exchange gas in the conduits which would result in a sluggish and undetermined conversion start.

The exchange reaction was running for four days. Regular measurements by laser Raman spectroscopy of gas phase and hydrate phase document the changes in relative guest molecule concentration. Also, structural changes in the hydrate phase could be detected by determining the Raman band position and the rate of cage occupancy. Thus, the Raman measurements also indicate the slow-down of the conversion process when no significant changes in the composition in the newly formed mixed hydrate occurred.

(3) After finishing the first conversion process, the durability of the newly formed CO_2-rich mixed hydrate has been tested by offering the initial hydrate-forming gas to this mixed hydrate. For that, the gas inflow route has been isolated again from the pressure cell and completely flushed with the hydrate-forming gas before re-opening of the inflow conduit. In similar manner, the rates of the return-conversion have been documented by laser Raman spectroscopy. The reaction proceeded for six to eight days.

4. Conclusions

The results of this study show, that small impurities in CH_4 gas hydrates or feed gas cause remarkable changes in the exchange behavior of gas hydrate molecules. With respect to the studied exchange reaction the influence of the tested impurities can be evaluated as follows:

7% C_2H_6 in CH_4 induces the formation of a sII hydrate which consequently results in structural changes during the course of molecule exchange reactions. Whereas the CH_4 release during the exchange reaction without structural conversion (e.g., CH_4-CO_2 exchange) amounts to about 50% after four days, the CH_4 release during the CH_4-C_2H_6–CO_2 exchange accounts for more than 85% in the same time span. Molecule exchange coupled to structural changes of the hydrate lattice causes not only an intense CH_4 release, but is also marked by a low CO_2 retention during a renewed offering of initial hydrate forming gas. The CO_2 retention of the simplest CO_2-CH_4 exchange experiment accounts for about 20% after seven days of exposition to CH_4. In contrast, the involvement of a structural conversion reduces the CO_2 retention to less than 10%.

1% SO_2 in CO_2 gas increases the stability of the resulting hydrate phase compared to simple CO_2 hydrate. The effect might be amplified by the tendency of SO_2 to accumulate within the hydrate lattice. We observed at the beginning of the exchange and reverse-exchange reaction a higher conversion rate, however, towards the end of the exchange the compositional values of the hydrates approach those resulting from exchange without SO_2. Therefore we conclude that the higher stability in terms of *p*-*T* conditions caused by SO_2 seems to influence only the induction of the exchange reaction but not the final result.

The study clearly demonstrates that the key driving force for the exchange process is the aim for equilibrium state of the chemical potential between all phases. The effectiveness of the molecule exchange in hydrates is well improved by structural changes (sI-sII) of the gas hydrates. The aim for thermodynamic stability in terms of *p*-*T* conditions has only a minor effect with respect to exchange processes and seems to influence particularly the start of the exchange.

Towards a scenario of gas production from natural hydrate formations by use of industrial CO_2, the influence of impurities can be valued positive with respect to CH_4 release. However, with respect to a secured long term storage option for CO_2 these results are challenging and show issues that need to be considered in numerical simulations and when exploring for an effective way of CH_4 recovery and CO_2 storage from/in gas hydrates.

Acknowledgments

We thank Manja Luzi for discussions and her help with the numerous Raman measurements. Also, BBS acknowledges the support of the HGF re-entry program that made this work possible.

References

1. Collett, T.S. *Energy Resource Potential of Natural Gas Hydrates*; AAPG Bulletin: Tulsa, OK, USA, 2002; Volume 86, pp. 1971–1992.
2. Max, M.D.; Johnson, A.H.; Dillon, W.P. *Economic Geology of Natural Gas Hydrate*; Springer: Berlin, Germany and Dordrecht, The Netherlands, 2006.
3. Soloviev, V.A. Global estimation of gas content in submarine gas hydrate accumulations. *Russ. Geol. Geophys.* **2002**, *43*, 609–624.
4. Klauda, J.B.; Sandler, S.I. Global distribution of methane hydrate in ocean sediment. *Energy Fuels* **2005**, *19*, 459–470.
5. Radler, M. World crude and natural gas reserves rebound in 2000. *Oil Gas J.* **2000**, *98*, 121–123.
6. Milkov, A.V. Molecular and stable isotope compositions of natural gas hydrates: A revised global dataset and basic interpretation in the context of geological settings. *Org. Geochem*. **2005**, *36*, 681–702.
7. Kvenvolden, K.A. A review of the geochemistry of methane in natural gas hydrate. *Org. Geochem.* **1995**, *23*, 997–1008.
8. Torres, M.; Wallmann, K.; Trehu, A.; Bohrmann, G.; Borowski, W.S.; Tomaru, H. Gas hydrate growth, methane transport, and chloride enrichment at the southern summit of Hydrate Ridge, Cascadia margin off Oregon. *Earth Planet. Sci. Lett.* **2004**, *226*, 225–241.
9. Matsumoto, R.; Takedomi, Y.; Wassada, H. Exploration of marine gas hydrates in Nankai Trough, Offshore Central Japan. Presented at AAPG Annual Convention, Denver, CO, USA, 3–6 June 2001.
10. Sassen, R.; Joye, S.; Sweet, S.T.; DeFreitas, D.A.; Milkov, A.V.; MacDonald, I.R. Thermogenic gas hydrates and hydrocarbon gases in complex chemosynthetic communities, Gulf of Mexico continental slope. *Org. Geochem*. **1999**, *30*, 485–497.
11. Lu, H.; Seo, Y.; Lee, J.; Moudrakovski, I.L; Ripmeester, J.A.; Chapman, N.R.; Coffin, R.B.; Gardner, G.; Pohlman, J. Complex gas hydrate from the Cascadia Margin. *Nature* **2007**, *445*, 303–306.
12. Aydin, G.; Karakurt, I.; Aydiner, K. Evaluation of geologic storage options of CO_2: Applicability, cost, storage capacity and safety. *Energy Policy* **2010**, *38*, 5072–5080.
13. Hendriks, C.; de Visser, E.; Jansen, D.; Carbo, M.; Jan Ruijg, G.; Davison, J. Capture of CO_2 from medium-scale emission sources. *Energy Procedia* **2009**, *1*, 1497–1504.
14. Ellis, B.R.; Crandell, L.E.; Peters, C.A. Limitations for brine acidification due to SO_2 co-injection in geologic carbon sequestration. *Int. J. Greenh. Gas Control* **2010**, *4*, 575–582.
15. Hirohama, S.; Shimoyama, Y.; Tatsuta, S.; Nishida, N. Conversion of CH_4 hydrate to CO_2 hydrate in liquid CO_2. *J. Chem. Eng. Jpn.* **1996**, *29*, 1014–1020.
16. Park, Y.; Kim, D.; Lee, J.; Huh, D.; Park, K.; Lee, J.; Lee, H. Sequestering carbon dioxide into complex structures of naturally occurring gas hydrates. *Proc. Natl. Acad. Sci. USA* **2006**, *103*, 12690–12694.
17. Schicks, J.M.; Luzi, M.; Beeskow-Strauch, B. The conversion process of hydrocarbon hydrates into CO_2 hydrates and *vice versa*: Thermodynamic considerations. *J. Phys. Chem. A* **2011**, *115*, 13324–13331.

18. Subramanian, S.; Kini, R.A.; Dec, S.F.; Sloan, E.D. Evidence of structure II hydrate formation from methane + ethane mixtures. *Chem. Eng. Sci.* **2000**, *55*, 1981–1999.
19. Beeskow-Strauch, B.; Schicks, J.M.; Spangenberg, E.; Erzinger, J. The influence of SO_2 and NO_2 impurities on CO_2 gas hydrate formation and stability. *Chemistry* **2011**, *17*, 4376–4384
20. Beeskow-Strauch, B.; Schicks, J.M.; Spangenberg, E.; Erzinger, J. Gas Hydrates as CH_4 source and CO_2 Sink—What do SO_2 Impurities Do? In *Proceedings of the EGU General Assembly*, Vienna, Austria, 19–24 April 2009.
21 Murshed, M.M.; Kuhs, W.F. Kinetic studies of methane–ethane mixed gas hydrates by neutron diffraction and Raman spectroscopy. *J. Phys. Chem. B* **2009**, *113*, 5172–5180.
22. Hester, K.C.; White, S.N.; Peltzer, E.T.; Brewer, P.G.; Sloan, E.D. Raman spectroscopic measurements of synthetic gas hydrates in the ocean. *Mar. Chem.* **2006**, *98*, 304–314.
23. Schicks, J.M.; Erzinger, J.; Ziemann, M.A. Raman spectra of gas hydrates differences and analogies to ice 1h and (gas saturated) water. Part A: Molecular and biomolecular spectroscopy. *Spectrochim. Acta* **2005**, 61, 2399–2403.
24 Kumar, R.; Lang, S.; Englezos, P.; Ripmeester, J.A. Application of the ATR-IR spectroscopic technique to the characterization of hydrates formed by CO_2, CO_2/H_2 and $CO_2/H_2/C_3H_8$. *J. Phys. Chem. A* **2009**, *113*, 6308–6313.
25. Sloan, E.D. *Clathrate Hydrates of Natural Gases*, 2nd ed.; M. Dekker Inc.: New York, NY, USA, 2008.
26. Ohno, H.; Strobel, T.A.; Dec, S.F.; Sloan, E.D.; Koh, C.A. Raman studies of methane-ethane hydrate metastability. *J. Phys. Chem. A* **2009**, *113*, 1711–1716
27. Hendriks, E.M.; Edmonds, B.; Moorwood, R.A.S.; Szczepanski, R. Hydrate structure stability in simple and mixed hydrates. *Fluid Phase Equilib.* **1996**, *117*, 193–200.
28. Burke, E.A.J. Raman microspectrometry of fluid inclusions. *Lithos* **2001**, *55*, 139–158.
29. Schrötter, H.W. Raman spectra of gases. In *Infrared and Raman Spectroscopy—Methods and Applications*; Schrader, B., Ed.; VCH Publishers, Inc.: New York, NY, USA, 1995; Chapter 4.3.2.3, p. 295.
30. Seitz, J.C.; Pasteris, J.D.; Chou, I.M. Raman spectroscopic characterization of gas mixtures. II. Quantitative composition and pressure determination of the CO_2–CH_4 system. *Am. J. Sci.* **1996**, *296*, 577–600.